Protection of 316L stainless steel by zirconia sol–gel coatings in 15% H_2SO_4 solutions

M. ATIK[+,*,0], C. R.'KHA[+], P. DE LIMA NETO*, L. A. AVACA*, M. A. AEGERTER*, J. ZARZYCKI[0]
[+]*Laboratoire de Chimie de Coordination, Université Cadi Ayyad Faculté des Sciences, Semlalia, Marrakech, Morocco,* [*]*Instituto de Física a Química de São Carlos, Universidade de São Paulo, Cx. Postal 369, 13560-970, São Carlos, SP, Brazil,* [0]*Laboratoire de Science des Matériaux Vitreux, Univerisité de Montpellier II, France*

Zirconia is a well known material which has excellent properties, such as high mechanical strength, chemical durability, alkali resistance, refractoriness, and can be used for chemical protection of metal substrates from attack by acid and oxidations [1–4]. The production of coatings by dip-coating is one of the most promising applications of the sol–gel process [5]. This method offers potential advantages over traditional techniques because coatings of various single component and multicomponent oxides have already been elaborated at low temperature.

Recently, the application of ultrasound irradiation during the preparation of the sols provided a new way to prepare a variety of gel, ceramics, glasses [6–8] and amorphous or crystalline coatings such as ZrO_2, SiO_2, SiO_2–TiO_2 and SiO_2–Al_2O_3 [9–14] showing improved properties over the traditional technique. All these coatings have been tested for chemical protection of 316L stainless steels against air corrosion, acid attack and in NaCl solutions, showing promising results.

The aim of this work is the preparation of ZrO_2 coated on a metallic substrate by dip-coating technique using a sol preparation involving sonocatalysis. The corrosion characteristics of the samples, either the bare substrate or coated with ZrO_2, were evaluated through potentiodynamic polarization curves obtained in deareated 15% H_2SO_4 solutions at 25, 40 and 50 °C.

The substrate used was 316L stainless steel of composition (wt %): 67.25 Fe, 18.55 Cr, 11.16 Ni, 2.01 Mo, 1.7 Mn, 0.026 Cu, 0.15 Si and 0.028 C. This material was chosen taking into account the heat treatment necessary for the densification of the coatings since this material has a low carbon content and is therefore less susceptible to sensitization (which in turn might promote enhanced corrosion).

Zirconium isopropoxide $Zr(OC_3H_7)_4$ diluted in isopropanol (C_3H_7OH) was used as the source of zirconia. Following the dissolution of the zirconium alkoxide in isopropanol, glacial acetic acid (CH_3COOH) was added to a solution homogenized with ultrasound irradiation 20 kHz (Heat Systems Ultrasonics W 385 sonicator) produced by a transducer immersed in the mixture. After 20 min, a homogeneous mixture was obtained. Excess of water was then added under ultrasound to complete the hydrolysis until a clear and transparent sonosol was obtained. The concentration of the starting alkoxide solutions was 0.5 mol/l and the volume ratios H_2O/C_3H_7OH and H_2O/CH_3COOH were, respectively, 1 and 2.

The as-received substrates were degreased ultrasonically in acetone. They were dipped into the solutions and withdrawn at a speed of 10 cm min^{-1} and then dried at 70 °C for 15 min. The samples were then heated to 400 °C at 5 °C/min for 1 h to remove organic residues, and oxidized in air at 800 °C with a heating rate of 5° min^{-1} to obtain adherent and dense coatings.

The resulting ZrO_2 thin-film structure was characterized by X-ray diffraction analysis using CuK_α radiation. Optical reflection spectra of the coated films were obtained with a Bomem FTIR spectrometer at an incident angle of 30°. The ZrO_2 surface was observed by scanning electron microscopy (Zeiss 960) and the film thickness was determined by ellipsometry (Rudolph – Automatic System).

Electrochemical measurements were carried out with freshly prepared samples in deareated 15% H_2SO_4 at different temperatures using a computerized PAR 273 Potentiostat/Galvanostat. A saturated calomel electrode (SCE) was used as reference and a Pt foil served as the auxiliary electrode. The working electrodes were immersed 1 cm in the solution. The potentiodynamic polarization curves were initiated at −0.7 V and scanned in the anodic direction at 1 mV s^{-1}. The data were analysed with the PAR model 342 Corrosion Measurements Software.

Fig. 1 shows X-ray diffractograms of the uncoated and coated substrates. Uncoated stainless steel shows three distinct peaks with d values of 0.208, 0.180 and 0.127 nm which correspond to the Cr + Fe + Ni cubic phase (Fig. 1a). After heat treatment at 800 °C for 2 h in air, the first peak decreases in intensity and other peaks appear with d = 0.364, 0.267 and 0.25 nm, corresponding to the formation of cubic and hexagonal Cr_2O_3 (Fig. 1b).

Stainless steel coated with ZrO_2 film and heat-treated at 800 °C for 2 h, shows the same three peaks seen in Fig. 1a (stainless steel uncoated as received) and one additional peak at 0.298 nm, corresponding to tetragonal zirconia (Fig. 1c). There is no change in relative intensity of the cubic metal peaks, indicating that no oxidation has occurred at the interface after the heat treatment.

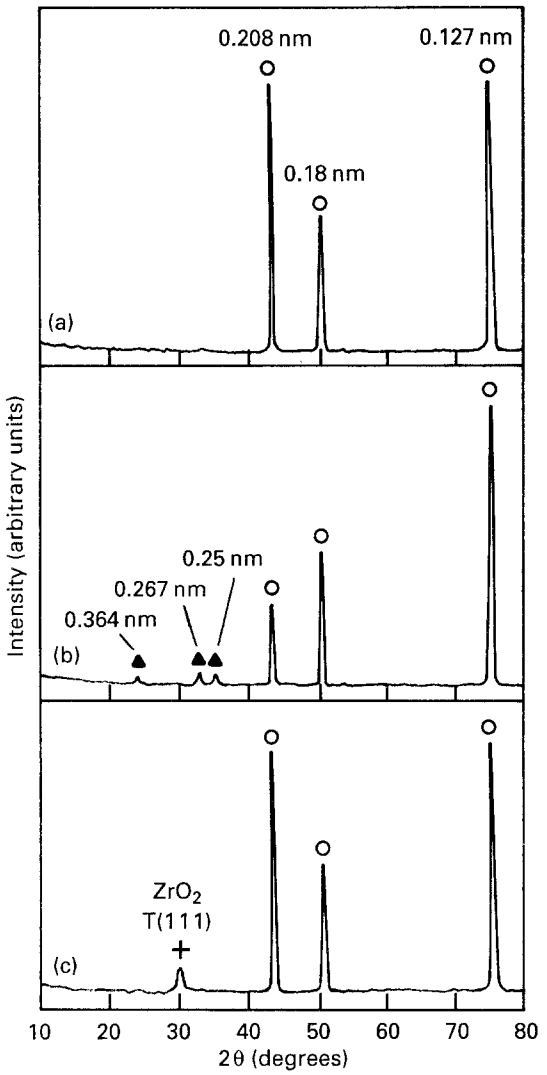

Figure 1 X-ray diffraction of stainless steel: (a) as received (uncoated); (b) uncoated but oxidized in air at 800 °C for 2 h; (c) ZrO_2-coated after oxidation at 800 °C for 2 h.

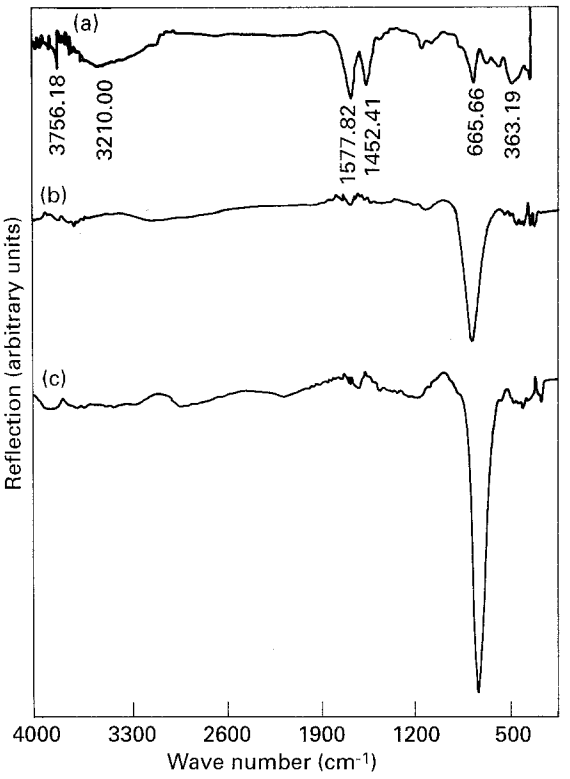

Figure 2 IR spectra of films prepared on stainless steel: (a) after deposition at room temperature; (b) ZrO_2-coated after densification at 800 °C for 1 h; (c) ZrO_2-coated after oxidation in air at 800 °C for 2 h.

Fig. 2 shows the evolution of the infrared spectra of the films deposited on stainless steel. At room temperature and before firing, the bands observed at about 1453–1578 cm^{-1} are characteristic of Zr–O–C species. Absorption bands due to Zr–O–Zr species are observed near 666 and 363 cm^{-1}. The evolution of the spectra with thermal treatment of the samples shows that the absorption due to Zr–O–C decreases and eventually disappears while that of Zr–O–Zr increases strongly with firing time and temperature.

Fig. 3 shows the microstructure of (a) untreated, (b) heat-treated stainless steel sheet surface and (c) a one-dip homogeneous ZrO_2 film, deposited on stainless steel. It was shown above that Cr_2O_3 crystals grow at the surface of heat-treated stainless steel heated at 800 °C for 2 h submitted to the same thermal treatment has ultrafine and dense microstructure. Scanning electron microscopy shows homogeneity of the coating.

The measurement of electrochemical corrosion in deareated 15% sulphuric acid was made with a film 0.5 μm thick; thicker coatings were shown to present cracks on the surface. Figures 4 to 6 show the results of potentiodynamic polarization curves obtained with uncoated and coated samples measured at 25, 40 and 50 °C.

The analysis of these results indicates that the coatings affect both the cathodic and anodic branches of the curves. In the cathodic branches, the slope of the cathodic reaction is maintained, but the values of the currents for the coated samples are smaller than the values for the uncoated samples, indicating that the corrosion mechanism remains unchanged and that the film acts, therefore, as a geometric blocking.

The anodic branches of the polarization curves show that the coatings have a strong effect on the current density in the passive region, diminishing the current value of uncoated and untreated stainless steel by roughly one order of magnitude, except for the polarization curve obtained at 50 °C, where the anodic current in the passive region is the same as that of uncoated but heat-treated stainless steel.

The combined cathodic and anodic effects of the coatings on the corrosion behaviour of 316L stainless steel are summarized in Table I. For instance, the corrosion rate (CR) of the coated stainless steel is about 8.4 times lower than that of substrates at 40 °C.

Sol–gel coatings of ZrO_2 prepared from sonocatalysed sols and deposited by a dip-coating technique on 316L stainless steel protect the metallic substrate against acid corrosion. The film is shown to act as a geometric blocking layer and increases the life-time of the substrate by a factor up to 8.4 at 40 °C. These oxide films can be used by the chemical and construction industries.

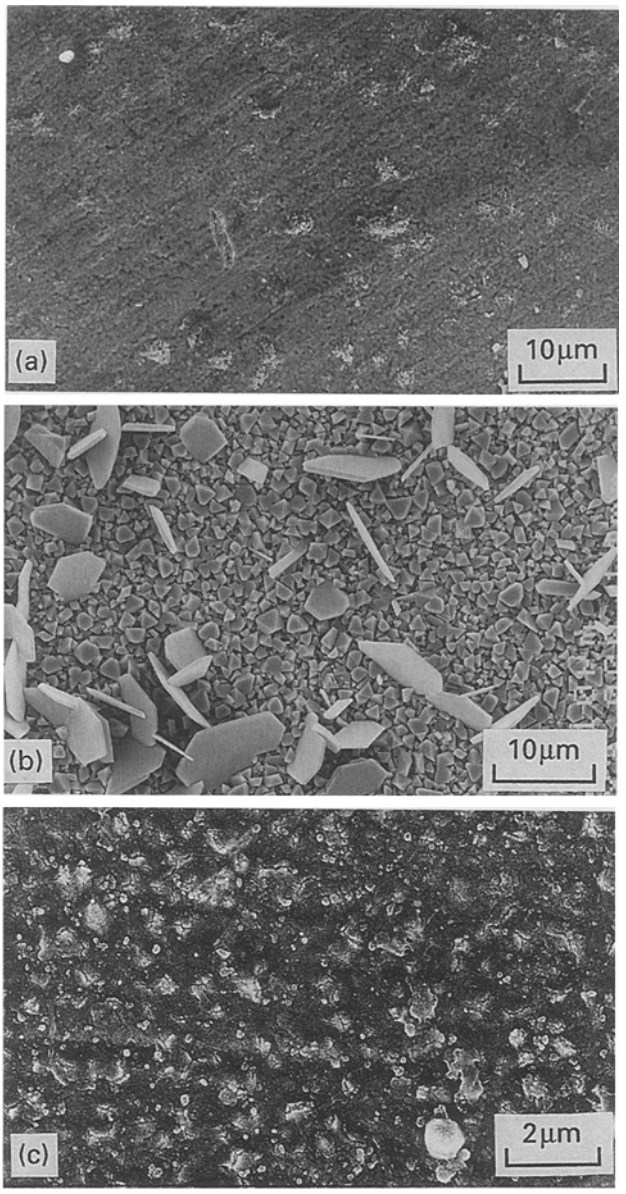

Figure 3 SEM micrograph of 316L stainless steel: (a) uncoated and untreated; (b) uncoated but heat-treated at 800 °C for 2 h; (c) coated with ZrO_2 (800 °C/2 h).

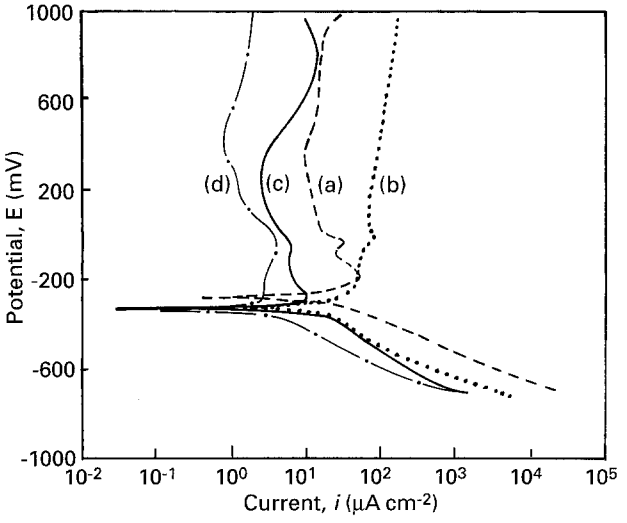

Figure 4 Potentiodynamic polarization curves measured in deareated 15% aqueous H_2SO_4 at 25 °C for 316L stainless steel: (a) uncoated and untreated; (b) uncoated but heat-treated at 800 °C for 2 h; (c) coated with ZrO_2 (800 °C/2 h); and (d) coated with ZrO_2 (800 °C/10 h).

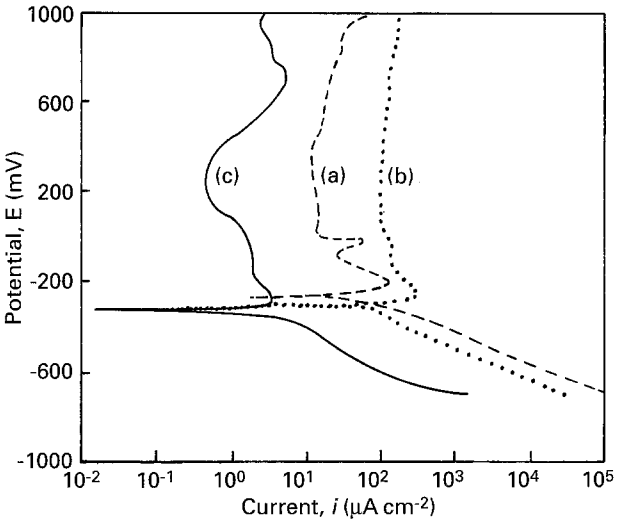

Figure 5 Potentiodynamic polarization curves measured in deareated 15% aqueous H_2SO_4 for 316L stainless steel: (a) uncoated and untreated; (b) uncoated but heat-treated at 800 °C for 2 h; (c) coated with ZrO_2 (800 °C/2 h) at $T = 40$ °C.

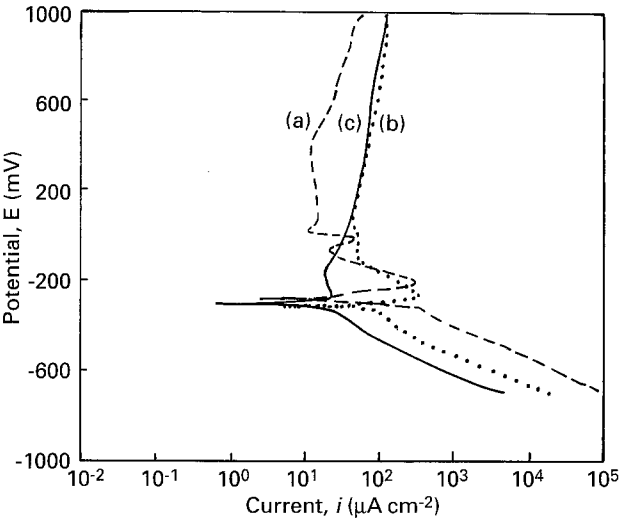

Figure 6 Same as Fig. 5, but at 50 °C.

TABLE I Corrosion parameters determined from the potentiodynamic curves measured for stainless steel 316L uncoated and untreated, uncoated but heat-treated at 800 °C/2 h and coated with ZrO_2 (800 °C/2 h), coated with ZrO_2 (800 °C/10 h): corrosion potential (E_{corr}), polarization resistance (R_p) and corrosion rate (CR)

Sample	T (°C)	$-E_{corr}$ (mV)	R_p (kΩ cm²)	CR (MPY)
	25	286	1.80	11.5
316L as received	40	261	0.37	35.2
	50	280	0.35	53.8
	25	306	1.45	5.0
316L heat-treated at	40	304	0.57	19.8
800 °C/2 h	50	307	0.14	41.2
	25	308	10.50	3.4
316L + ZrO_2 coating	40	328	8.50	4.2
(800 °C/2 h)	50	299	0.99	12.9
316L + ZrO_2 coating	25	328	9	3
(800 °C/10 h)				

Acknowledgements

This research was sponsored by FAPESP, FINEP, CNP_q, CAPES/PICD and the Program RHAE-Novos Materials (Brazil).

References

1. N. TOHGE, A. MATSUDA and T. MINAMI, *Chem. Expr.* **2** (1987) 141.
2. L. YANG and J. CHANG, *J. Non-Cryst. Solids* **112** (1989) 442.
3. D. GANGULI and D. KUNDU, *J. Mater. Sci. Lett.* **3** (1984) 503.
4. K. SUGIOKA, H. TASHIRO, K. TOYODA, H. MURAKAMA and H. TAKAI, *J. Mater. Res.* **5** (1990) 2835.
5. H. DISLICH, *J. Non-Cryst. Solids* **63** (1984) 237.
6. N. DE LA ROSA-FOX, L. ESQUIVIAS and J. ZARZYCKI, *Rev. Phys. Appl.* **24 Coll. C4** (1989) 233.
7. M. PINERO, M. ATIK and J. ZARZYCKI, *J. Non-Cryst. Solids* **147&148** (1992) 523.
8. N. DE LA ROSA-FOX, L. ESQUIVIAS and J. ZARZYCKI, in "Effects of modes of formation on the structure of glass", in Proceedings of 2nd International Conference Nashville, TN, June, edited by R. A. Weeks and D. L. Kinser (Trans. Tech. Aedermannsdorf, 1987) p. 363.
9. M. ATIK and M. A. AEGERTER, *J. Non-Cryst. Solids* **147&148** (1992) 813.
10. M. ATIK and M. A. AEGERTER, *Mater. Res. Soc. Symp. Proc.* **271** (1992) 471.
11. M. ATIK, C. R'KHA and J. ZARZYCKI, *J. Mater. Sci. Lett.* **13** (1994) 266.
12. P. DE LIMA NETO, M. ATIK, L. A. AVACA and M. A. AEGERTER, *J. Sol–Gel Sci. Technol.* **1** (1994) 177.
13. M. ATIK and J. ZARZYCKI, *J. Mat. Sci. Lett.* (1994).
14. P. DE LIMA NETO, M. ATIK, L. A. AVACA and M. A. AEGERTER, VIIth International Workshop on Glasses and Ceramics from Gels, Paris, 1993, *J. Sol–Gel Sci. Technol.* (1994) (accepted).